THE ASTROPHYSICAL JOURNAL, 336:367–375, 1989 January 1

REDSHIFTS DERIVED FROM GAMMA-RAY BURST SPECTRA ARE INCONCLUSIVE

WŁODZIMIERZ KLUŹNIAK[1]
Physics Department, Stanford University
Received 1988 April 4; accepted 1988 June 21

ABSTRACT

If the reported large widths of the "annihilation" features in gamma-ray burst spectra are real, the inferred value of the redshift can be as high as $z = 0.8$, depending on the emission mechanism. A model is presented in which a broad annihilation line peaking at 400 keV corresponds to a Doppler blueshift of the emitting region of $z = -0.3$. The prevalent view that the observed line centers of burst annihilation features imply emission from the surface of a nonrotating neutron star is not supported by the available data. However, emission from *rapidly rotating neutron stars* is a viable possibility.

Subject headings: gamma rays: bursts — radiation mechanisms — stars: neutron

I. INTRODUCTION

Reporting the discovery of emission features in gamma-ray burst (GRB) spectra, Mazets *et al.* (1980) interpreted them as gravitationally redshifted e^+e^- annihilation lines. Since a redshift value of $z = 0.25$ was inferred for the canonical 400 keV peak, the emission features are taken as evidence that the bursts originate in neutron stars. Indeed, in accordance with the Schwarzschild formula $1 + z = (1 - 2GM/Rc^2)^{-1/2}$, the characteristic ratio of mass to linear dimension of the source would be $1\ M_\odot/10$ km. The proponents of a cosmological GRB origin challenge this widely accepted interpretation, disputing the alleged clustering of the emission feature peak energy about the value of 400 keV. Furthermore, they demonstrate that it is possible to obtain a hard emergent photon spectrum from plasma optically thick to pair creation *provided* there is no observable annihilation peak (Paczyński 1986; Goodman 1986).

Although the very presence of annihilation lines in GRB spectra is controversial (Nolan *et al.* 1983, 1984; Golenetskii *et al.* 1986; Fenimore *et al.* 1982), I will take their existence for granted. For a review of GRB issues see Liang and Petrosian (1986). The purpose of this paper is to examine whether the peak energies of the GRB annihilation features do in fact imply emission from the surface of static neutron stars. To this end I will confront observations with simple annihilation models. In the Appendix, evidence for a correlation between the peak energies and half-widths of the features is discussed. In § II, the range of redshifts inferred from the features in the context of the three models discussed is shown to be surprisingly large. The value of z is found to be model dependent.

The question whether the "annihilation" features exclude a cosmological origin of gamma-ray bursts cannot be addressed until a systematic, bias-free survey of the 100 keV to a few MeV energy range of a large number of GRB spectra is carried out. The issue considered here is whether the inferred redshifts of the features reported to date are consistent with GRBs originating in neutron stars and whether in fact a neutron star origin is preferred by the best available values of z.

Recently Liang (1986) addressed even more specific issues in an attempt to constrain the properties of the nuclear equation of state. Although his compilation includes an impressive number of annihilation features, his conclusions are weakened by the *a priori* exclusion of redshifts larger than 0.7 or smaller than 0.02. Furthermore, the method of continuum subtraction by eye is not free of bias, and Liang's sample includes spectra in which the presence of emission features is controversial (Nolan *et al.* 1984), on equal footing with those confirmed by many spacecraft. For these reasons Liang's conclusion that there is a definite clustering of redshifts between 0.2 and 0.5 does not seem secure, although it is more cautious than the earlier claim by Mazets *et al.* (1981) that $z \approx 0.2$–0.3. Also, in the absence of an emission model constraining the region of line formation to be at the stellar surface any derived redshift value will only yield a lower limit to the surface redshift.

Nevertheless, the quoted range of z values is significant in the following sense. Define z_0 by the equation

$$1 + z_0 \equiv mc^2/E_0 , \tag{1}$$

where mc^2 is the electron rest energy and E_0 is the location of the peak of the emission line whose shape is derived by subtracting the continuum from the detected photon number spectrum $N(E)$. The true value E_t, at which the photon spectrum peaks, and the true line shape are uncertain because the derived values of E_0 and Δ_0, the full width at half-maximum (FWHM) of the emission feature, depend on the continuum subtraction method used. Also the spectrum $N(E)$ deconvolved from raw counting data is not unique. Indeed, Fenimore *et al.* (1982) have shown that a Comptonized blackbody spectral fit can be made for GB 781104 which removes all traces of the "annihilation feature." Finally, the spectrum quality is often degraded by poor counting statistics. These are precisely the reasons why Liang needed a large sample for his study. There may also be an intrinsic spread of the true value E_t. I interpret Liang's (1986) result

$$0.2 \leq z_0 \leq 0.5 , \tag{2a}$$

or rather the corresponding energy range

$$340\ \text{keV} \leq E_0 \leq 425\ \text{keV} , \tag{2b}$$

to be a statement of the most probable range of *observational* uncertainty in the value of E_t.

It is well known (e.g. Harding 1986) that the relevant annihilation emission mechanisms produce source spectra $R(E)$ which usually peak at energies $E_s \geq mc^2$. The photon number flux density at the source, $F(E)$, is related in a definite manner

[1] On leave of absence from Copernicus Astronomical Center of the Polish Academy of Sciences, Warsaw.

to the flux density at a distant location, $F_d(E)$, which in turn is related to the observed photon spectrum:

$$N(E) \propto \iint F_d(E)\, dt\, dA\ , \tag{3}$$

the integration extends over the effective area and integration time of the detector. The detected redshift z is then given by the formula

$$1 + z = E_s/E_0\ . \tag{4}$$

It is often tacitly assumed that the difference between equations (1) and (4) is unimportant in view of the large observational uncertainties, equation (2). I will show that this is not the case.

II. MODELS OF e^+e^- EMISSION

In most of the following I assume that the discussed emission features are, in fact, due to e^+e^- annihilation and that the values of E_0 and Δ_0 (§ I) have been accurately determined. For purposes of comparison with theoretical models, the empirical values of E_0 and Δ_0 discussed in the Appendix are assumed here to reflect true properties of GRB spectra in the solar system crossing spacetime region. The main conclusion of the Appendix is that the width of the features correlates with, and is in fact comparable to, the energy value at which the emission features peak.

Clearly, since both E_0 and Δ_0 are a function of the unknown redshift, it is convenient to consider the relativistic invariant

$$\frac{E_s}{\Delta_s} = \frac{E_0}{\Delta_0}\ , \tag{5}$$

where the subscript s refers to the line properties at the source.

The work of Zdziarski (1984*a*, *b*, 1986) shows that the spectra of optically thick pair-equilibrium thermal plasmas do not exhibit annihilation features. This constrains emission models considerably. Below I discuss the values of E_s/Δ_s predicted by three simple models.

a) Thermal Plasma

The hypothesis of thermal broadening of annihilation lines formed in the absence of a magnetic field is worth examining.

Table 1 lists the peak energies E_s and the FWHMs Δ_s of pure annihilation spectra $R(E)$ of Ramaty and Mészáros (1981). Golenetskii *et al.* (1986) realize that those values are incompatible with their E_0, Δ_0, and $z = z_0$ (eq. [1]), and make an *ad hoc* suggestion that the spectrum is a superposition of emission from layers of different temperatures. However, it is difficult to see how that could lead to a significant broadening of the line without inducing a corresponding shift in E_s.

TABLE 1

SPECTRAL PROPERTIES OF OPTICALLY THIN THERMAL PLASMAS[a]

T (K)	E_s (keV)[b]	Δ_s (keV)[c]	E_s/Δ_s
3×10^8	530	210	2.5
1×10^9	570	370	1.5
3×10^9	700	850	0.8
1×10^{10}	1250	2500	0.5

[a] According to Figs. 2 and 3 of Ramaty and Mészáros 1981.
[b] The photon spectrum peaks at energy E_s.
[c] Δ_s is the FWHM of the photon spectrum.

TABLE 2

REDSHIFTS INFERRED FROM GRBS ACCORDING TO THREE MODELS

Event (1)	T or B (2)	$1 + z_t$ (3)	$1 + z_0$ (4)	$1 + z_+$ (5)
GB 781006b	10^9 K	1.2	1.02	0.54
GB 781104b[a]	10^9 K	1.4	1.25	0.68
GB 781119[a]	0.8×10^9 K/1×10^9 K	1.3/1.3	1.20	0.69[b]
GB 781119[a, c]	$\geq 10^{13}$ G	1.4	1.20	0.69[b]
GB 781119[d]	10^{10} K	2.7[e]	1.09	0.57
GB 790116	2×10^9 K	1.5	1.19	0.63
GB 790418	1.6×10^9 K	1.8	1.46	0.77
GB 790613	3×10^9 K	1.8	1.25	0.68

Col. (1): Refer to Table 3 for the properties of emission features in the GRB events.

Col. (2): The value of the temperature was obtained by setting $E_s/\Delta_s = E_0/\Delta_0$ (see Tables 1 and 3).

Col. (3): z_t is the redshift derived from the thermal model with parameters as in col. (2); the redshift for the strong magnetic field model of GB 781119 is also given (see §§ II*a*, II*b*).

Col. (4): The naive redshift factor z_0 is defined in eq. (1).

Col. (5): Col. (5) gives the blueshift, eq. (4), according to the in-flight annihilation model with $E_s = 270$ keV (see § II*c*).

[a] Signe data; see Table 3.

[b] Both the 420 keV and the 740 keV line can be due to annihilation if the values $E_s = 290$ keV and $E_s = 511$ keV are used, respectively, for the two lines. For these values the redshift is $z_+ = -0.31$, as given. $E_s = 270$ keV would have given $1 + z_+ = 0.64$ for the 420 keV line.

[c] ICE data for the 740 keV line; see Table 3.

[d] Konus data; see Table 3.

[e] Probably the sum of two unresolved lines.

The entries in column (2), Table 2, are obtained by correlating (see eq. [5]) the reported values of E_0/Δ_0 (Table 3) with E_s/Δ_s (Table 1), graphically interpolating the latter values when necessary. Column (3) shows the inferred redshift of the source (eq. [4]). The large value $z = 1.7$ for GB 781119 is unlikely to be real as remarked in the Appendix ($\Delta_0 \neq 990$ keV?), and is omitted from further discussion. All the inferred values of z are much larger than the corresponding values z_0. Furthermore, the same value of $E_0 = 400$ keV corresponds to two very different redshifts of $z = 0.4$ for GB 781104b and $z = 0.8$ for GB 790613. Note that these are the very two events whose spectra are most reliable (see Table 3, and references). Of the six redshifts z_t, two ($z = 0.8$) are incompatible with any of the Arnett and Bowers (1977) static neutron star models, and one ($z = 0.5$) implies the star is near its maximum mass limit (see Lindblom and Detweiler 1983). However, the *causal* upper bound on the gravitational redshift from the surface of a static neutron star is higher, $z \leq 0.9$ (Lindblom 1984), and can accommodate all six values of z_t (but not the suspect value 1.7).

The highest possible redshift for a rotating neutron star modeled with standard equations of state requires backward equatorial emission and is $z_b = 2.3$, comfortably above all the entries in Table 3, column (3) (Friedman, Ipser, and Parker 1986). However, it is hard to imagine a mechanism that would allow only backward emission from the equator. The observed peak would most likely have to be the edge of a broad emission feature, occurring between $E_s/(1 + z_b)$ and $E_s/(1 + z_f)$, with intensity $EN(E) \propto E^4$, where z_b and z_f are the backward and forward redshifts, respectively; this is not observed. Another possibility is polar emission from rapidly rotating neutron stars. The polar redshifts of the maximum mass uniformly rotating models of Friedman *et al.* are typically $z_p \approx 0.6$–0.7

(and $z_p = 1.89$ for the ultrasoft Friedman-Pandharipande equation of state); at the highest rotation rates $z_p = 0.77$ is reached for some models.

Inclusion of Compton scattering is not likely to lead to a broadening of the annihilation peak. The work of Zdziarski (1984*b*) indicates that this would require a very contrived set of parameters. In the examples exhibited in his paper Compton scattering either wipes out the annihilation peak completely or does not change the FWHM appreciably. This is due to the large fractional energy change in a typical Compton scattering of 500 keV photons, which tends to reduce the flux of a narrow peak without broadening it.

I conclude that optically thin thermal emission at $T \sim 10^9$ K can explain large line widths but requires large values of redshift. Compatibility with the neutron star paradigm and standard equations of state can be achieved only if rapid rotation is admitted.

b) Strong Magnetic Fields

For field values $B < 10^{12}$ G and at emission angle (with respect to the field direction) $\theta = \pi/2$ corresponding to the largest FWHM, the 2-γ annihilation spectrum, $R(E)$ (see eq. [3]), of an e^+e^- pair at rest has a symmetric shape peaking at $E_s = mc^2$ (Daugherty and Bussard 1980). The inferred redshift is z_0 (eq. [1]) and is listed in column (4) of Table 2. The problem with this interpretation of the origin of the emission feature widths is that $\Delta_s \leq 100$ keV, i.e. the FWHM is far below any value of Δ_0 ever reported in a GRB (for the energy range 100 keV $\leq E_0 \leq$ 500 keV). Thermal broadening cannot be invoked to impart large widths to annihilation lines formed in a region of strong magnetic field because the longitudinal cooling rate exceeds the annihilation rate at $B = 10^{12}$ G already at $T = 10^7$ K (Katz 1982). One way to obtain a significant broadening of the line would be to allow emission from a tall column, i.e. a region spanning a range of elevations, in which case z_0 would be a lower limit to the surface redshift. (The redshift of the base of the emitting column could be obtained by replacing E_0 in eq. [1] with E_r, the lowest value of energy at which emission is significantly higher than the continuum [i.e. the edge of the red wing].) Another difficulty is that no correlation is expected between E_s and Δ_s unless the field value $B \geq 10^{13}$ G, i.e. unless the 1-γ annihilation process becomes important.

For $B = 10^{13}$ G, the widest 2-γ peak is observed at the angle $\theta = \pi/2$ with $\Delta_s \approx 300$ keV and $E_s \approx 550$ keV. The only width in the 1-γ peak is due to thermal broadening and, at $\theta = \pi/2$, $E_s = 1020$ keV. The existence of two peaks and their width ratio is compatible with the *ISEE* 3 data for GB 781119, assuming $kT \approx 10^6$ K; the inferred redshifts (eq. [4]), are $z_2 = 0.3$ and $z_1 = 0.4$ for the 420 keV and the 740 keV lines, respectively. A value $B_s > 10^{13}$ G can be found at which the two redshifts agree, $z_1 = z_2 = 0.4$, because, for $\theta = \pi/2$, $E_s = 2mc^2$ for the 1-γ process at any value of B, while $E_s < 2mc^2$ and $dE_s/dB > 0$ for the 2-γ annihilation. The angle θ is quite constrained because $dE_s/d\theta$ has the opposite sign for the two processes. The width Δ_s varies strongly with θ for the 2-γ process, so in general it may not be possible to match both the redshifts and the widths, should another example of a burst with two lines be discovered.

I conclude that the 420 keV and 740 keV lines reported for GB 781119 by *ISEE 3* are compatible (as first suggested by Katz 1982) with annihilation lines formed in a magnetic field of strength $B > 10^{13}$ G at a redshift of $z = 0.4$. If this is the origin of the two lines, GB 781119 would be a special object, because the large observed widths Δ_0 of the annihilation features and the apparent correlation between E_0 and Δ_0 lend no support for the hypothesis that in other bursters, in which only a single annihilation feature is seen, the reported annihilation line originates in a region of strong magnetic field. However, if that hypothesis were nevertheless true with $B < 10^{12}$ G, z would be equal to z_0 (see eq. [1] and Table 2).

c) In-Flight Annihilation

i) *The Spectrum*

It is quite likely that positrons produced by GRB mechanisms will be accelerated to relativistic energies, just as the solar flare positrons are (Ramaty, Kozlovsky, and Lingenfelter 1975). Such acceleration is certainly expected in Sturrock's (1986) GRB flare model and in Ruderman's (1987) evacuated magnetosphere scenario. Relativistic positron production has also been invoked in other astrophysical contexts: in accretion tori around black holes (cascade production, Blandford 1982) and in intense radiation fields (photon-photon production, Lingenfelter and Ramaty 1982); relativistic positrons are also expected to be produced in pulsars (Sturrock 1971; Cheng, Ho and Ruderman 1986*a*, *b*) and in the magnetospheres of accreting neutron stars (Kluźniak *et al.* 1988).

An energetic positron beam may traverse a layer of fluid and emerge from it without thermalizing or it may penetrate a target so deeply that annihilation "at rest" will occur at large optical scattering depths. In either of these two special cases only the e^+e^- pairs which annihilate in flight will contribute to the annihilation spectrum and the energy E of the emitted photons is constrained by simple kinematical considerations to be in the range:

$$E_b \leq E \leq E_f \,, \tag{6}$$

$$E_b = \frac{mc^2}{1+\beta_c} \approx \frac{mc^2}{2}\left(1 + \frac{1}{2\gamma_+}\right), \tag{7a}$$

$$E_f = \frac{mc^2}{1-\beta_c} \approx mc^2\left(\gamma_+ + \frac{1}{2} - \frac{1}{2\gamma_+}\right). \tag{7b}$$

The approximate equalities on the extreme right of equations (7a) and (7b) hold in the extreme relativistic (ER) limit, i.e., when the energy of the incoming positron exceeds the electron rest mass,

$$E_+ = \gamma_+ mc^2 \gg mc^2 \,. \tag{8}$$

The lower limit, E_b, is attained by photons emitted backward ($\mu \equiv \cos\theta = -1$), while E_f corresponds to photons emitted forward ($\mu = +1$). In fact, there is a unique relationship between the photon energy and the angle of observation:

$$E = \frac{mc^2}{1-\mu\beta_c} \,. \tag{9}$$

Here β_c is the velocity of the positron-electron center of mass system in the laboratory (LAB) frame which is defined to be the rest frame of the electron (and the target),

$$\beta_c = \left(\frac{\gamma_+ - 1}{\gamma_+ + 1}\right)^{1/2} \,. \tag{10}$$

The angular average of the photon annihilation spectrum $R(E)$ emitted by a monochromatic beam of positrons impinging upon electrons at rest has been computed by Svensson

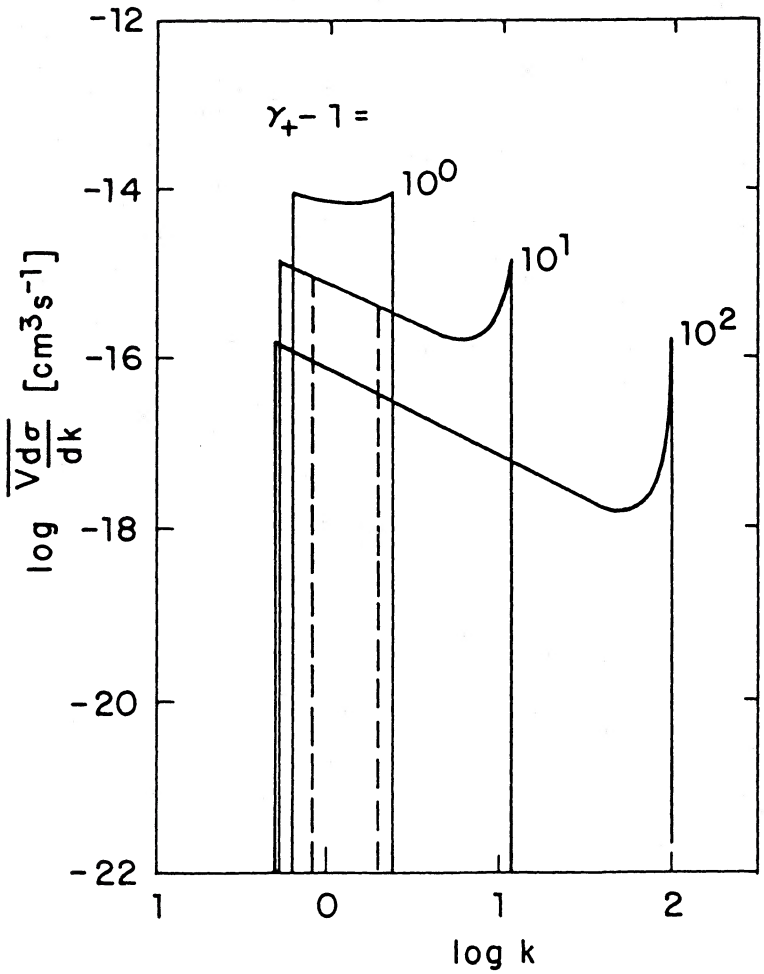

FIG. 1.—Adapted from Svensson (1982). The angle averaged emissivity of positrons of energy $E_+ = \gamma_+ mc^2$ annihilating in flight with electrons at rest. Dotted lines show the effect of restricting the direction cosine between the positron momentum vector and the line of sight to some range $\mu_1 \leq \mu \leq \mu_2$, implying a restriction on the observed photon energies $E_1 \leq E \leq E_2$ (see eqs. [18a]–[18f]). In the figure, $k \equiv E/mc^2$ is the photon energy in units of electron rest mass.

(1982) and is reproduced here as Figure 1. The minimum in the spectrum corresponds to photons emitted at right angles to the beam direction in the center of mass (CM) frame. In the LAB frame this energy is

$$E_T = \frac{mc^2}{1-\beta_c^2} . \tag{11}$$

For relativistic positrons, $\gamma_+ \gg 1$, and for photon energies less than E_T the spectrum has the simple sawtooth shape

$$R(E) = \Theta(E-E_b)\left(\frac{E}{E_b}\right)^{-1} R_0 , \quad E < E_T . \tag{12}$$

Here Θ is the Heaviside step function and $R_0 = R(E_b) = R(E_f)$ is the peak photon spectral intensity. The last equality, i.e., the fact that the forward and backward peaks have equal strength, follows from momentum conservation in the CM frame. In the CM frame the photons are emitted in narrow backward and forward cones; the annihilation cross section for the backward cone is, in the ER limit,

$$\frac{d\sigma_{+-}}{d\Omega_{\rm CM}} \approx \frac{r_0^2(1-\beta_c^2)}{2(1-\beta_c^2\,\mu_{\rm CM}^2)} . \tag{13}$$

The transformation of the angles between CM and LAB frames,

$$d\mu_{\rm LAB} = (1-\beta_c\,\mu)^2(1-\beta_c^2)^{-1}\,d\mu_{\rm CM} , \tag{14}$$

gives the characteristic E^{-1} dependence of the LAB cross section and of the photon number spectrum $R(E)$, for $\mu_{\rm CM} \approx -1$,

$$\frac{d\sigma_{+-}}{dE} \approx \frac{2\pi r_0^2}{(\gamma_+ + 1)\beta_c}\frac{E_b}{E}(mc^2)^{-1} . \tag{15}$$

Here $r_0^2 = e^2/(mc^2)$ is the classical electron radius, and equations (7a), (9) and (10) were used. The E^{-1} dependence of $R(E)$ leads to the relation $R(2E_b) = R(E_b)/2$; i.e. the FWHM is equal to the peak energy

$$E_s = E_b , \tag{16a}$$

$$\Delta_s = E_s . \tag{16b}$$

Equation (16b) is precisely the content of hypothesis H_2, which is shown in the Appendix to be in agreement with the data from GRB observations. The conditions for validity of equations (16a) and (16b) are that the beam of positrons is rela-

tivistic with $\gamma_+ \gtrsim 3$ and that the spectrum is averaged over the background hemisphere (a semiring will suffice due to the azimuthal symmetry); i.e. that angles in the range

$$-1 \leq \mu \leq \mu_{\max}\ , \quad 0 \leq \mu_{\max}\ , \tag{16c}$$

are allowed. Note that the value of E_b is not very sensitive to the value of γ_+. The peak energy, E_b, equations (16a) and (7a), can be observed as E_0 if the whole system including the rest frame of the target (LAB) electrons is boosted, giving a Doppler redshift of

$$1 + z_+ = E_b/E_0\ . \tag{16d}$$

For a specific value of $E_+ = 5.1$ MeV,

$$\gamma_+ = 10\ , \quad E_b = 0.53mc^2 = 270\ \text{keV}\ , \tag{17a}$$

and the photon energy at the minimum of the spectrum (eq. [11]), is $E_T = 5.3$ MeV seen at an angle of 26° from the forward direction of the beam. The backward peak at $E_s = E_b$ (equation [17a]) corresponds to a redshift

$$1 + z_+ = 270\ \text{keV}/E_0\ , \tag{17b}$$

and this value is given in the last column of Table 2.

Within the context of the neutron star GRB paradigm the required angular average over the range (eq. [16c]) can be obtained if azimuthal symmetry (about the stellar axis) of the beam, which is assumed to be lying in the equatorial plane, is postulated or if time averaging of the emission of a rapidly rotating source is performed. Values of z_+ down to a blueshift of $z_f = -0.32$ can be explained by forward equatorial emission of rapidly rotating neutron stars (Friedman, Ipser, and Parker 1986), but larger values of the blueshift, i.e. $z_+ < -0.32$ would be an embarassment. For a rotating star one naturally expects equatorial emission in all directions with redshift values anywhere in the range $z_f \leq z \leq z_b$, but this only leads to a smoothing out of the peak and its slight broadening since the observed feature would then be a convolution of sawtooth peaks of strength proportional to E_z^{-3}, where $E_z = E_b(1 + z)^{-1}$ (see discussion in § II*a*). In passing, let us note that a spread in the energies of the annihilating positrons would also lead to a slight blunting of the jagged sawtooth of Figure 1, but would not otherwise affect any of the other conclusions, as long as all positron energies are relativistic $\gamma_+ \gg 1$. Thus, the positron beam need not be monochromatic in this discussion.

The peak energy can be increased and/or the FWHM can be decreased if a different range of viewing angles is allowed,

$$\mu_{\min} \leq \mu \leq \mu_{\max}\ , \tag{18a}$$

with the corresponding minimum and maximum energies (see eqs. [9], [10]),

$$E_{\min} = mc^2(1 - \beta_c\,\mu_{\min})^{-1}\ , \quad E_{\max} = mc^2(1 - \beta_c\,\mu_{\max})^{-1}\ . \tag{18b}$$

If $E_{\max} < E_T$ (eq. [11]), the spectrum is a tooth obtained by shrinking the support of the function R (eq. [12] or Fig. 1), to the interval $(E_{\min}, E_{\max})$,

$$R_1(E) = \Theta(E - E_{\min})\Theta(E_{\max} - E)R(E)\ . \tag{18c}$$

This is illustrated by the dotted lines in Figure 1. The peak energy E_s and the FWHM, Δ_s, are now

$$E_s = E_{\min}\ , \tag{18d}$$

$$\Delta_s = \min\,(E_s, E_{\max} - E_{\min})\ . \tag{18e}$$

Equation (18d) corresponds to a redshift

$$1 + z = (1 - \beta_c\,\mu_{\min})^{-1}(1 + z_0)\ , \tag{18f}$$

where z_0 is given by equation (1), so an annihilation peak observed at E_0 can correspond to an arbitrary redshift $z \geq z_+$ (see eqs. [16a], [16d] and [7a]), if only the viewing angle is suitably restricted and the energy $\gamma_+ mc^2$ of the positrons in the beam is high enough.

ii) *Conditions under Which the In-Flight Annihilation Peaks May Be Seen*

The energy loss rate of a positron of speed $v_+ = \beta_+ c$ traversing a medium of total electron density n is (Kihara and Aono 1963; Frankel, Hines, and Dewar 1979)

$$-\frac{dE_+}{dt} = \frac{4\pi ne^4}{mv_+}\ln\left(\frac{2mv_+^3}{\gamma e^2\omega_p}\right)\ . \tag{19}$$

Here e is the electron charge, $\omega_p = (4\pi e^2 n/m)^{1/2}$ is the plasma frequency, and $\ln\gamma = 0.57\ldots$.

The stopping length, $l = c(\gamma_+ mc^2)(dE_+/dt)^{-1}$ of a relativistic positron will exceed the target thickness D when the Thomson scattering depth τ_{es} is less than 2.6% of γ_+:

$$\frac{D}{l} \approx \tau_{es}\left(\frac{\gamma_+}{40}\right)^{-1}(1 - 0.02\ln n_{14}) \ll 1\ ; \tag{20}$$

here n_{14} is the total electron density in units of 10^{14} cm^{-3}. Alternatively, the positrons will stop after traversing a layer of scattering depth $\tau_{es} \gg 1$ if

$$\gamma_+ = 40\tau_{es}(1 - 0.02\ln n_{14}) \gg 40\ . \tag{21}$$

In either case the "511" keV annihilation peak of thermalized positrons would not be seen. The former case could correspond to positrons traversing a cloud of plasma surrounding a central object. The latter case could occur when high-energy positrons hit the surface of a neutron star. In this case the forward peak of Figure 1 (see eq. [7b]) would never be seen. Note that the mean total scattering angle is (Jackson 1975)

$$\langle\Theta^2\rangle \approx 0.3Z\tau_{es}\left(\frac{\gamma_+}{10}\right)^{-2}\ , \tag{22}$$

i.e., $\langle\Theta^2\rangle \ll 1$ under the conditions discussed. Here Z is the (suitably averaged) atomic number of the element(s) constituting the medium.

If $\gamma_+/40 < \tau_{es} < 1$ both the in-flight annihilation emission and the much stronger thermal annihilation peak should be seen. See § II*c*(iii), for a further discussion of this point.

The emissivity due to in-flight annihilation is

$$L_{+-} = (2 + \gamma_+)mc^3 n_+ n\sigma(\gamma_+)\ , \tag{23a}$$

where $\sigma(\gamma_+)$ is the Heitler total LAB annihilation cross section and n_+ is the positron density in the beam. In the extreme relativistic limit

$$\frac{L_{+-}}{n_+ n} \approx \pi r_0^2 mc^3[\ln(2\gamma_+ + 2) - 1]\ . \tag{24}$$

The bremsstrahlung emissivity of a relativistic positron beam is (Alexanian 1968)

$$\frac{L_{\text{ff}}}{n_+ n} = 4\alpha(Z + 2)r_0^2 mc^3(\gamma_+ + 1)\left[\ln(2\gamma_+ + 2) - \frac{1}{3}\right]\ , \tag{25a}$$

where $\alpha \approx 1/137$ is the fine-structure constant. For $\gamma_+ = 10$

and $Z = 1$, equations (23) and (25) give

$$\frac{L_{+-}}{n_+ n} = 2.2 \times 10^{-14} \text{ cm}^3 \text{ s}^{-1} \ (mc^2)$$
$$= 1.8 \times 10^{-20} \text{ ergs cm}^3 \text{ s}^{-1} , \quad (23b)$$

$$\frac{L_{\text{ff}}}{n_+ n} = 6.3 \times 10^{-15} \text{ cm}^3 \text{ s}^{-1} \ (mc^2)$$
$$= 5.3 \times 10^{-21} \text{ ergs cm}^3 \text{ s}^{-1} , \quad (25b)$$

Note that the in-flight annihilation emissivity given by equation (23b) is comparable with that of a 10^9 K thermal, optically thin plasma (Ramaty and Mészáros 1981), while the peak intensity, R_0 (eq. [12]), of the emissivity spectrum is (see eq. [15] or Fig. 1)

$$R_0 = mc^3 \frac{d\sigma_{+-}}{dE} \approx 1.5 \times 10^{-15} n_+ n \text{ cm}^3 \text{ s}^{-1} ; \quad (23c)$$

i.e., $\sim 10\%$ of the peak value of the thermal spectrum at $T = 10^9$ K.

For $\gamma_+ = 10$ and $Z = 1$ the bremsstrahlung emissivity can be neglected; at any rate it only contributes to the smooth continuum. Even at higher values of γ_+ or Z, when $L_{\text{ff}} > L_{+-}$, the backward annihilation peak is not washed out. In the ER limit the LAB frame annihilation cross section is

$$\frac{d\sigma_{+-}}{dE} = \frac{2\pi r_0^2}{\gamma_+ + 1} \frac{E_b}{E} (mc^2)^{-1} = 0.6 r_0^2 (mc^2)^{-1} , \quad (26)$$

for $E = E_b, \gamma_+ = 10$.

The positron-ion bremsstrahlung cross section

$$\frac{d\sigma_Z^{\text{ff}}}{dE} = 4Z^2 \alpha r_0^2 (E)^{-1} \left[1 + \left(\frac{E_+ - E}{E_+} \right)^2 - \frac{2}{3} \right]$$
$$\times \left[\ln \frac{2E_+(E_+ - 1)}{mc^2 E} - \frac{1}{2} \right] = 0.4 Z^2 r_0^2 (mc^2)^{-1} , \quad (27)$$

for $E = E_b, \gamma_+ = 10$, and $Z = 1$, can be appreciable but all the emission is beamed in a narrow forward cone of opening angle $\theta \sim mc^2/E_+$. In collision with an electron, the positron radiates in the narrow forward cone too, with the cross section (for $Z = 1$)

$$\frac{d\sigma_+^{\text{ff}}}{dE} = \frac{d\sigma_Z^{\text{ff}}}{dE} . \quad (28)$$

However, the electron also radiates and the relevant cross section is

$$\frac{d\sigma_-^{\text{ff}}}{dE} = \frac{2}{3} \alpha r_0^2 (mc^2)^{-1} \left(\frac{mc^2}{E} \right)^2 \left[\left(4 - \frac{m}{E} + \frac{m^2}{4E^2} \right) \ln \left(\frac{2E_+}{m} \right) \right.$$
$$\left. - 2 + 2 \frac{m}{E} - \frac{5m^2}{8E^2} \right] = 0.17 r_0^2 (mc^2)^{-1} , \quad (28b)$$

for $E = E_b, \gamma_+ = 10$, but this is seen to be less than the annihilation cross section (eq. [26]). Furthermore, although the electron radiates into the narrow backward cone in the CM frame, this radiation gets isotropized in the LAB frame, so the bremsstrahlung cross section for radiating a photon of energy E_b in the backward direction is a fraction of the value given by equation (28b). Although the backward annihilation cone also is isotropized in the LAB frame, the photon energy in the CM frame is fixed and hence photons of energy E_b in the LAB frame are seen only in the backward direction $\mu = -1$ (see eqs. [7], and [9]).

In conclusion, a beam of relativistic positrons of energy $E_+ = \gamma_+ mc^2$ traversing a medium of scattering depth τ_{es}, satisfying equations (20) or (21), will not give rise to the usual peak of thermalized annihilation "at rest." Instead, it will lead to the spectrum of Figure 1. The strength of the bremsstrahlung continuum is less than that of the annihilation peak for values of $\gamma_+ \lesssim 30$ and for viewing angles in the backward direction this remains true for even greater positron energies. For $\gamma_+ = 10$ the peak spectral annihilation intensity is $\sim 10\%$ of the "511" keV annihilation line of thermalized positrons in plasma of temperature $T \geq 10^6$ K (Bussard, Ramaty, and Drachman 1979; Lingenfelter and Ramaty 1982) and 10% of the annihilation rate at 10^9 K. However, the total emissivity given by equation (23) is comparable to the emissivity at 10^9 K.

iii) *Implications for GRB Emission Features*

In those bursts in which only one ("400 keV") emission feature is seen, z_+ as determined in Table 2 can be tentatively identified with the rotational blueshift of the neutron star. (Strictly speaking, as seen from eq. [18], $z_+ \leq z$. However, especially in the view of the observation that $E_0 = \Delta_0$, there seems no reason to assume that the viewing angle is restricted, as would be required for $z_+ \neq z$.)

Outside the neutron star paradigm, the blueshift can be imagined to be due to expansion of a plasma as in Paczyński's (1986) and Goodman's (1986) proposals, although it is not at all apparent how to arrange for outgoing plasma and ingoing positrons.

For a single observed peak, the redshifts cannot be determined quite accurately from equations (4), (16a), and (7a), the positron energy being a free parameter. However, both z and E_+ can in principle be determined uniquely in those rare cases when the spectrum shows two peaks. This is illustrated by the case of GB 781119. The positron beam can explain the 740 keV line as a blueshifted ($z = -0.31$) 511 keV line. The 420 keV line in the same burst corresponds to the in-flight annihilation peak seen at the same blueshift ($z = -0.31$), provided that in the LAB frame $E_s = 290$ keV. Assuming $E_s = E_b$, this implies $\gamma_+ = 3.7$ (eq. [7]). Thermal emission from plasma at temperature $10^6 \text{ K} \leq T \leq 10^9$ K gives annihilation rate $R_{\text{th}} \approx 1 \times 10^{-14} \text{ cm}^3 \text{ s}^{-1} \ n_+ n$ (Ramaty and Mészáros 1981; Bussard, Ramaty, and Drachmann 1979). The backward hemisphere photon emission rate due to annihilation in flight (eqs. [23c], [12], and [7a] is $R_{+-} \approx 2 \times 10^{-15} \text{ cm}^3 \text{ s}^{-1} \ n_+ n$. The ratio $R_{\text{th}}/R_{+-} \approx 5$ is in good agreement with the ratio of line strengths of the 740 keV and the 420 keV lines reported to be 6.1 (Teegarden and Cline 1980). If $T < 10^7$ K the intrinsic width of the 511 keV line is small, FWHM < 30 keV (40 keV for the blueshifted width). If the Doppler blueshift $z = -0.31$ of the peaks is due to forward equatorial emission in a rapidly rotating neutron star, and the emission is isotropic, convolution of narrow lines emitted at different angles along the equator would lead to a feature of profile $N(E) \propto E^3$, as discussed previously. For the 740 keV line this leads to a FWHM $\Delta_0 = 190$ keV in good agreement with the value of 180 keV quoted in Table 3.

Unfortunately the profile asymmetry of the blueshifted 511 keV line is in the wrong sense: neutron star rotation would lead to a 570–760 keV feature instead of the 720–900 keV

reported.[2] However, there is no reason to expect isotropic emission from the thermalized positrons. Equation (20) shows that for $\gamma_+ = 3.7$ the positron beam penetrates only down to scattering depth $\tau_{es} \approx 0.1$. Annihilation occurs in an optically thin layer and a significant limb brightening is expected, $F(E, \theta) \propto |\cos \theta|^{-1}$ for $|\cos \theta| \geq 0.1$.

III. CONCLUSIONS

In the absence of a systematic search for gamma-ray burst features in a wide energy range (at least 100 keV to several MeV) no firm conclusions can be drawn about the existence and origin of e^+e^- annihilation lines. Taken by themselves, the spectral emission features cannot, at present, be used to exclude a cosmological origin of classic GRBs. The most fruitful approach right now is to assume that GRBs are associated with neutron stars and to use the properties of emission features to constrain specific models of gamma-ray bursts. The emission features with peak energies $E_0 \approx 300$–500 keV reported in some spectra of gamma-ray bursts (Table 3) are broad ($\Delta_0 \approx$ several hundred keV) and often rapidly variable on time scales limited by instrumental resolution. The published data are in good agreement with the hypothesis (H_2) that $\Delta_0 = E_0$. In contrast, the hypothesis (H_5 of the Appendix) that there is no correlation between the reported FWHM Δ_0 and the line "center" E_0 of the emission features can be rejected at a confidence level better than 0.05.

If these results are not an artifact of the fitting procedures, they may indicate that the $\sim$400 keV emission feature is due to in-flight annihilation of relativistic positrons traversing a plasma which moves toward the observer with a velocity corresponding to a Doppler blueshift of $z \approx -0.3$. In this context, the peak energies of the reported GRB emission features may be taken as evidence of rapid rotation of the underlying neutron star. I further suggest that the narrow 740 keV line in GB 781119 is a blueshifted 511 keV annihilation line, with the same redshift value $z = -0.3$.

I could not find any other simple emission model which would give $E_0 \approx \Delta_0$. In any case, mechanisms that would lead to significant line widths, such as thermal broadening or emission from a tall column, tend to give redshift values much larger than the value $z \approx 0.3$ previously quoted in the literature. In some cases, the redshifts obtained (Table 2) exceed values permitted for static neutron stars modeled with conventional equations of state.

Clearly, it would be (at the very least) premature to conclude that the "annihilation" lines in the spectra of classic GRBs originate at the surface of a nonrotating neutron star. In fact, emission features provide no direct evidence for neutron star origin of GRBs, although *rapidly rotating* neutron stars are not excluded as the site of their origin. High-quality data on the properties of the emission features, particularly the line shape, are needed before any firm conclusions can be drawn about the strength of the gravitational field in the region of emission. A clear understanding of the gamma-ray burst mechanism may also be necessary before an unambiguous redshift value can be deduced from the annihilation emission features.

I would like to thank Dr. Andrzej Zdziarski for an informative discussion and for comments on the manuscript. I also benefited from a conversation with Professor Vahé Petrosian and from Professor Robert V. Wagoner's careful reading of the manuscript. Professor Bohdan Paczyński and Dr. Eric Linder are thanked for commenting on the manuscript. This work was supported in part by NASA grant NAGW-299 and NSF grant PHY 86-03273. The cost of publication was defrayed by NSF grant AST-86-02831.

[2] Of course, the statistical significance of the line shape is lower than that of the occurrence of the line itself; in any case, neither the line shape nor its width was explained by the original suggestion that the line is nuclear in origin.

APPENDIX

GAMMA-RAY BURST EMISSION FEATURES

It is important to establish the typical observed properties of the purported annihilation line. The ratio of the line center to its width is of particular importance (see eq. [5]). For illustrative purposes consider a sample of six gamma-ray burst spectra (Table 3) whose properties are particularly well established. An important omission is the famous GB 790305b event, which exhibited a prominent emission line at 430 keV with full width half-maximum (FWHM) $\approx$ 150 keV (Mazets *et al.* 1982), the smallest ever reported (in this energy range) for a GRB spectrum and, in fact, the only one with FWHM less than 200 keV. However, it is clear that GB 790305b was unique in other respects as well (Cline 1980); together with two or three other members, its source belongs to the distinct class of soft gamma-ray repeaters.

The six events listed in Table 3 are the only ones which satisfy the following three criteria:

1) The event is a "classic" burst (it is not associated with a known repeater);
2) The "annihilation" feature has been reported in spectra detected by two or more different spacecraft;
3) E_0 (defined following eq. [1]) and Δ_0 ($\equiv$FWHM of the feature after continuum subtraction) has been reported, together with some measure of the statistical significance of the spectral fit.

I. THE GOLENETSKII *et al.* RESULTS

Four of the sets of values in Table 3 come from the extensive report of Golenetskii *et al.* (1986), therefore it is important to discuss their method. The Golenetskii list contains fits to 39 spectra of 19 bursts, but if duplicate spectra yielding the same values of (E_0, Δ_0) are discarded, the remaining "full" sample contains $n = 28$ spectra. It is worth noting that often the (E_0, Δ_0) values are stable when the parameters of the continuum component $dN_c/dE \propto E^{-\gamma} \exp(-E/kT)$ vary considerably. The best values of E_0 and Δ_0 correspond to the minimum χ^2 value obtained in fitting the spectrum with a sum of two components, the continuum dN_c/dE and the line $dN_l/dE \propto E^\alpha/[E^\beta + (\epsilon mc^2)^\beta]$, but only that minimum value of χ^2_q is reported by Golenetskii *et al.* (q = number of degrees of freedom), so it is impossible to assess the statistical significance of the alleged emission line, much less that of the reported best values

TABLE 3

MOST RELIABLY ESTABLISHED EMISSION FEATURES IN "CLASSIC" GAMMA-RAY BURSTS

Burst	Spacecraft/Experiment	$\alpha/(\beta-\alpha)$[a]	E_0[b]	Δ_0[c]	E_0/Δ_0	Significance[d]	Reference
GB 781006b	V-11, V-12/KONUS	3.5/3.5	500	380	1.3	$\chi^2_{24}=23$	1
GB 781104b	V-11, V-12/Signe	Gaussian	400	270	1.5	$C=0.999$	2
	V-11, V-12/KONUS		400[e]	...[e]	...	...	3
GB 781119	V-11, V-12/KONUS	2/1.2	470	990	0.47	$\chi^2_8=13$	1
	V-11, V-12/Signe	...	420	280/~250[f]	1.5/1.7[f]	significant/probable[f]	4
	ISEE 3	...	420	"broad"	...	1.4 σ	5
	ISEE 3	...	740	90–180[g]	8.–4.	3.45 σ, $C=0.993$	5, 6
GB 790116	V-11, V-12/KONUS	2.6/2.6	430	450	0.96	$\chi^2_{22}=23$	1
GB 790418	V-11, V-12/KONUS	3.2/3.2	350	300	1.2	$\chi^2_{23}=24$, $C=0.95$	1
GB 790613	V-11/KONUS	2/2.4	400	510	0.78	$\chi^2_7=8$	1
	PVO & V-11, V-12/Signe	...	...	...	...	...	1[h], 7[h]

[a] Parameters describing the line shape. See the Appendix or reference 1 for details.
[b] E_0 is the energy at which $N(E)$ peaks after subtraction of continuum.
[c] $\Delta_0 \equiv$ FWHM of the residual peak.
[d] The significance refers to the existence of the line, not its particular parameters E_0, Δ_0.
[e] Data shown in graphic form; Δ_0 seems to be in agreement with the Signe value. Golenetskii *et al.* also report an emission feature in the *Konus* spectra of this Nov 4 burst, they give several fits with Δ_0 ranging from 280 to 520 keV with $E_0 = 370$ keV (reference 1).
[f] Values for different spectra from the same burst.
[g] The FWHM has not been reported in reference 5, but the line is discussed variously as a "narrow" line and the "720–900" keV feature.
[h] The spectra are in good agreement with the *Konus* spectra.

REFERENCES.—(1) Golenetskii *et al.* 1986. (2) Barat *et al.* 1984*b*. (3) Mazets *et al.* 1980, 1981a. (4) Barat 1983. (5) Teegarden and Cline 1980. (6) Vestrand 1986. (7) Barat *et al.* 1984*a*.

of the parameters (E_0, Δ_0) derived. Here α, β, and ϵ were three of the seven free parameters fitted. This fitting method is quite different from the conventional continuum subtraction used by Barat *et al.* (1984*b*), among others, who search systematically for emission features by comparing χ^2_q obtained by fitting the function $dN/dE = A\{E^{-\gamma}\exp(-E/E_1) + B\exp[-(E-E_0)^2/\Delta_0)^2]\}$ with value $B = 0$ and with value $B \neq 0$, thus allowing an assesment of the confidence level C at which the emission feature is seen. Due to this difference as well as the different line shapes assumed, the sample in Table 3 is not homogeneous.

It is possible that the large widths reported by Golenetskii *et al.* are an artifact of the fitting method, but how this may arise is not obvious. Their values of E_0/Δ_0 vary between 0.71 and 1.3, with additional single points at 0.38, 0.47, and 1.9. Taking the "full" sample of $n = 28$ spectral fits, let us examine two hypotheses regarding the random variable $X = E_0/\Delta_0$:

Hypothesis H_1: the extreme values $x_1 = 0.38$ and $x_2 = 1.9$ are compatible with a Gaussian distribution of X with (unknown) mean m and (unknown) dispersion σ^2.

Hypothesis H_2: the mean value of X is $m = 1$.

The sample of 28 values of x_i gives $\bar{x} \equiv n^{-1}\sum_{i=1}^{n} x_i = 1.05$, and $nS^2 \equiv \sum_{i=1}^{n}(x_i - \bar{x})^2 = 2.05$. Student's t-test with 27 d.o.f. yields

$$0.95 < m < 1.15\,,$$

with probability $P = 0.98$. The χ^2 test for 27 d.o.f. leads to $\sigma^2 < 0.418$ with $P = 0.999$ and $\sigma^2 < 0.26$ with $P = 0.95$.

Hypothesis H_1 can be rejected at a level better than 10^{-3} for the point x_1 and better than 10^{-4} for the point x_2. The corresponding widths, 940 keV and 200 keV, must be flukes—indeed, other statistically more significant fits are also reported for the same bursts with $0.9 \leq E_0/\Delta_0 \leq 1.1$. Assuming the value of m is not known *a priori*, there is no reason to reject hypothesis H_2, even at the 0.1 confidence level. If hypothesis H_2 is understood as a prediction of $m = 1$, the agreement with the data is very good: $\chi^2_{28} = 2.1$ for all points, or $\chi^2_{26} = 1.3$ if the extreme points x_1, x_2 are discarded.

Clearly, the Golenetskii sample of 28 spectra favors $0.95 < E_0/\Delta_0 < 1.15$, the hypothesis H_2 gives an excellent fit, and the 1 σ range of E_0/Δ_0 is 0.5–1.6. The possibility that $E_s \approx \Delta_s$ needs to be taken very seriously.

II. EVIDENCE FOR $E_s = \Delta_s$ IN THE WELL-ESTABLISHED FEATURES

In the smaller sample of reliable spectra (Table 3) GB 781119 merits particular attention. The 740 keV line has only been seen in the *ISEE 3* (ICE) data and was originally attributed to the 847 keV iron line (Teegarden and Cline 1980). Clearly, the extraordinary width of the 470 keV line reported by the *Konus* group may be due to the presence of an unresolved 740 keV line.

Putting aside the 740 keV line, and taking $\Delta_0 = 250$ keV and $E_0 \doteq 420$ keV for the other GB 781119 line, an analysis of the sample of $n = 6$ spectra thus obtained reveals $\bar{x} = 1.2$, $nS^2 = 0.92$. Hypothesis H_2 yields $\chi^2_6 = 0.92$, and hence it cannot be rejected at the $P = 0.01$ level. If m is taken not to be known *a priori*, Student's test gives

$$0.73 < m < 1.67\,, \qquad \text{with } P = 0.98\,. \tag{A1}$$

One can also test the following additional hypotheses:

Hypothesis H_3: the distribution of E_0 is flat (uniform);
Hypothesis H_4: the distribution of Δ_0 is flat (uniform);
Hypothesis H_5: there is no correlation between E_0 and Δ_0.

The hypothesis H_5 can be rejected at the 0.04 confidence level, while there are no grounds for rejecting any of the hypotheses H_2, H_3 and H_4. This contradicts the prevailing assumption that the emission features correspond to a well-defined E_s and a well-defined redshift (eq. [4]), and that the operative line broadening mechanisms lead to various widths Δ_s for the same peak energy E_s of emission. Clearly the reverse is true: there is a correlation between the reported values of E_0 and Δ_0, and there is no evidence for any single preferred value of E_0. I ignore the possibility that these results may be an artefact of the fitting procedure or of observer bias. If in fact $E_s/\Delta_s = m$ is constant, the preferred value is given by equation (A1).

The *a priori* assumption that $E_s/\Delta_s = 1.0$ leads to excellent agreement with the data, provided the observed dispersion $\sigma^2 < 0.365$ ($P = 0.95$), can be explained by instrumental resolution and fitting uncertainties.

REFERENCES

Alexanian, M. 1968, *Phys. Rev.*, **165**, 253–257.
Arnett, W. D., and Bowers, R. L. 1977, *Ap. J. Suppl.*, **33**, 415–436.
Barat, C. 1983, in *Proc. AIP Conf. 101, Positron-Electron Pairs in Astrophysics*, ed. M. L. Burns, A. K. Harding, and R. Ramaty (New York: AIP), pp. 54–58.
Barat, C., *et al.* 1984*a*, *Ap. J.*, **280**, 150–153.
———. 1984*b*, *Ap. J. (Letters)*, **286**, L11–L13.
Blandford, R. D. 1982, in *Proc. AIP Conf. 83, The Galactic Center*, ed. G. R. Riegler and R. D. Blandford (New York: AIP), pp. 177–179.
Bussard, R. W., Ramaty, R., and Drachman, R. J. 1979, *Ap. J.*, **228**, 928–934.
Cheng, K. S., Ho, C., and Ruderman, M. 1986*a*, *Ap. J.*, **300**, 500–521.
———. 1986*b*, *Ap. J.*, **300**, 522–539.
Cline, T. L. 1980, *Comments Ap.*, **9**, 13–22.
Daugherty, J. K., and Bussard, R. W. 1980, *Ap. J.*, **238**, 296–310.
Fenimore, E. E., Klebesadel, R. W., Laros, J. G., Stockdale, R. E., and Kane, S. R. 1982, *Nature*, **297**, 665–667.
Frankel, N. E., Hines, K. C., and Dewar, R. L. 1979, *Phys. Rev. A*, **20**, 2120–2129.
Friedman, J. L., Ipser, J. R., and Parker, L. 1986, *Ap. J.*, **304**, 115–139.
Golenetskii, S. V., Mazets, E. P., Aptekar, R. L., Guryan, Yu. A., and Ilyinskii, V. N. 1986, *Ap. Space Sci.*, **124**, 243–278.
Goodman, J. 1986, *Ap. J. (Letters)*, **308**, L47–L50.
Harding, A. K. 1986, in *Proc. AIP Conf. 141, Gamma-Ray Bursts*, ed. E. P. Liang and V. Petrosian (New York: AIP), pp. 126–127.
Jackson, J. D. 1975, *Classical Electrodynamics* (New York: Wiley).
Katz, J. I. 1982, *Ap. J.*, **260**, 371–385.
Kihara, T., and Aono, O. 1963, *J. Phys. Soc. Japan*, **18**, 837–851.
Kluźniak, W., Ruderman, M., Shaham, J., and Tavani, M. 1988, CAL-352 preprint.
Liang, E. P. 1986, *Ap. J.*, **304**, 682–687.
Liang, E. P., and Petrosian, V., eds. 1986, *Proc. AIP Conf. 141, Gamma-Ray Bursts* (New York: AIP).
Lindblom, L. 1984, *Ap. J.*, **278**, 364–368.
Lindblom, L., and Detweiler, S. 1983, *Ap. J. Suppl.*, **53**, 73–92.
Lingenfelter, R. E., and Ramaty, R. 1982, in *Proc. AIP Conf. 83, The Galactic Center*, ed. G. R. Riegler and R. D. Blandford (New York: AIP), pp. 148–159.
Mazets, E. P., Golenetskii, S. V., Aptekar', R. L., Gur'yan, Yu. A., and Il'inskii, V. N. 1980, *Pis'ma Astr. Zh.*, **6**, 706–711 (English transl. in *Soviet Astr. Letters*, **6**, 372–375 [1980]).
———. 1981*a*, *Nature*, **290**, 378–382.
Mazets, E. P., *et al.* 1981*b*, *Ap. Space Sci.*, **80**, 119–143.
Mazets, E. P., Golenetskii, S. V., Guryan, Yu. A., and Ilyinskii, V. N. 1982, *Ap. Space Sci.*, **84**, 173–189.
Nolan, P. L., Share, G. H., Chupp, E. L., Forrest, D. J., and Matz, S. M. 1984, *Nature*, **311**, 360–362.
Nolan, P. L., Share, G. H., Forrest, D. J., Chupp, E. L., Matz, S. M., and Rieger, E. 1983, in *Proc. AIP Conf. 101, Positron-Electron Pairs in Astrophysics*, ed. M. L. Burns, A. K. Harding, and R. Ramaty (New York: AIP), pp. 59–63.
Paczyński, B. 1986, *Ap. J. (Letters)*, **308**, L43–L46.
Ramaty, R., Kozlovsky, B., and Lingenfelter, R. E. 1975, *Space Sci Rev.*, **18**, 341.
Ramaty, R., and Mészáros, P. 1981, *Ap. J.*, **250**, 384–388.
Ruderman, M. 1987, in *Proc. 13th Texas Symposium on Relativistic Astrophysics*, ed. M. Ulmer (Singapore: World Scientific), pp. 448–459.
Sturrock, P. A. 1971, *Ap. J.*, **164**, 529–556.
———. 1986, *Nature*, **321**, 47–49.
Svensson, R. 1982, *Ap. J.*, **258**, 321–332.
Teegarden, B. J., and Cline, T. L. 1980, *Ap. J. (Letters)*, **236**, L67–L70.
Vestrand, T. 1986, in *Proc. AIP Conf. 141, Gamma-Ray Bursts*, ed. E. P. Liang and V. Petrosian (New York: AIP), p. 106.
Zdziarski, A. A. 1984*a*, *Ap. J.*, **283**, 842–847.
———. 1984*b*, *Phys. Scripta*, **T7**, 124–126.
———. 1986, *Ap. J.*, **303**, 94–100.

WŁODZIMIERZ KLUŹNIAK: Physics Department, Columbia University, New York, NY 10027